

# Investigation of realizing SDI with high swirl charge in a motorcycle engine

Yuh-Yih Wu, Hsien-Chi Tsai, Manh-Cuong Nguyen

**Abstract**—The targeted developments for future vehicles are how to reduce fuel consumption, pollutant emission while maintaining high level of engine performance. To deal with those issues, fuel system has been taken great concerns by scientists for a long period of time. As we know, Port Fuel Injection system (PFI) and Gasoline Direct Injection system (GDI) are popular techniques which are being used on commercial vehicles. This paper presents the possible improvement of engine performance by applying effect of swirl motion on lean-limit of semi-direct injection SI engine. The fuel goes into cylinder directly through intake valve near the middle intake stroke to make richer mixture around the spark plug, which is called semi-direct injection (SDI). Thus, this system includes high swirl charge, injection during intake valve opening, and air-assisted fuel injection. The modifications of intake port by using baffle plate and the other by closing one intake valve for the 125 cc, 4-valve, port-fuel-injection (PFI) engine to increase swirl ratio of in-cylinder air motions which helped to form rich mixture around spark plug, and lean mixture at other location which is so-called stratified charge. The CFD software was used to investigate the in-cylinder air motion. After that, the combustion characteristics of swirl charge were investigated. The SDI engine then was tested under lean conditions at 4500 rpm and 5300 rpm. Experimental results indicated that lean-limit was extended to maximum air-fuel ratio 25.26 (excess air ratio = 1.73) at swirl ratio 3.5 while brake specific fuel consumption and coefficient of cycle variation were very low. Finally, the ECE-40 driving cycle simulation was employed for lean burn SDI engine as well as the original PFI engine. Results show that by using SDI mode at low engine load operation of ECE-40 driving cycle, the fuel consumption, CO emission, and NO<sub>x</sub> emission were improved by 4%, 31.1%, and 5.9%, respectively. However, the HC emission was increased by 25%.

**Keywords**—CFD, Lean burn, Semi-direct Injection System, Swirl ratio

## I. INTRODUCTION

**I**N order to postpone the energy crisis, one method is to employ the alternative fuels [1]-[3], another is to reducing the fuel consumption of internal combustion engine (ICE), and the other is to use electric power. In addition, the global warming effect is an important concern as well. However, the design of an internal combustion engine is a complex compromise between performance, fuel economy and emissions. These three factors are interrelated and they can not be simultaneously optimized. By making an engine more efficient, one or more of these factors could be increased without significantly compromising the others.

Thus, studies related to internal combustion engine have been being vigorously investigated in spacious areas such as

fuel injection development, exhaust emission treatment and especially the engine operating can have low emissions and high efficiency [4]-[5] to achieve the targeted values. In addition, engine running at lean condition will have low pumping work because of throttle wide opening. However, the disadvantage of lean burn is the instability of combustion that can be improved by using stratified charge [6].

Many researches have been taken to improve fuel injection characteristics by examining available problems and developing new systems. For example, the improvement of gasoline direct injection (GDI) has solved disadvantages of traditional multi-point injection (MPI) system. Fry et al. [7] showed that positioning the fuel injector is the key consideration for GDI engine which improved engine performance at full-loaded operation comparing to MPI system. Moreover, the study also proved that Air Assist low pressure GDI (AAGDI) was more flexible in its operation at part load, tolerating greater ranges of injection timing, air fuel ratio (AFR) and exhaust-gas recirculation (EGR), whilst maintaining stable combustion.

The weak point of such systems is their structural complexity and high production costs. Nevertheless, it is still possible to built very simple systems on some components of stratified charge combustion system. A lean-burn system with catalytic pre-chamber that made possible unfailing ignition and flame development of the lean charge included in main combustion chamber was presented by Jarosinski et al. [8]. The other method – semi-direct injection (SDI) system which is previously developed on 2-stroke SI engine [9]-[10] indicated that SDI could decrease engine emissions while maintaining its performance and improving idle operating condition by stabilizing the combustion, minimizing cyclic variation. The main motivations for swirl ratio in lean burn of semi-direct injection SI engine applications are to lower the exhaust emissions and to improve the power density or performance of engine.

Therefore, this study focused on operating the SDI on a motorcycle engine with high swirl charge. Strong swirl motion interferes mixing of air so that the fuel distributed in the upper area at early compression stage may occupy the upper portion of mixture i.e. near the spark plug position until the end of compression, which was so-called stratified charge. Therefore, relatively richer mixture is distributed around the spark plug and this promotes ignition ability and early initial flame stability [11]. From above obtain, lean-limit can be increased by increasing swirl motion and mixture around spark plug.

Therefore, a concept of SDI system with high swirl motion on engine performance was examined.

## II. EXPERIMENTAL SETUP

### A. Target Engine

This study used a 125cc single-cylinder motorcycle engine as a target engine, which was produced by SANYANG Industry Co., Ltd. Detail specifications of the target engine are shown in Table I.

TABLE I: ENGINE SPECIFICATIONS

Engine Type	124.6cc, Air Cooled
Valve System	4 Valves - SOHC
Bore x Stroke	52.4mm×57.8mm
Compression Ratio	10.5:1
Compression Pressure	12±2 kg/cm <sup>2</sup>
Max Power	10.1ps/8500rpm
Max Torque	0.93kg-m/7000rpm
Ignition System	Direct-current crystal
Fuel System	EFI, port injection
Intake Valve Open*	10°BTDC
Intake Valve Close*	20°ABDC
Exhaust Valve Open*	30°BBDC
Exhaust Valve Close*	10°ATDC
* Valve timing is defined at 1mm of valve lift.	

### B. Fuel Atomization system

Because the fuel of SDI is injected into cylinder directly through intake valve, the fuel atomization becomes a concern. To improve the fuel atomization, an air-assisted fuel injection system produced by KYMCO (Kwang Yang Motor Co., Ltd.) was used. The adapter of Air-assisted Injection includes 3 major components as shown in Fig. 1 (1) Fuel injector; (2) The mixing chamber provides the link to the compressed air circuit that is used to force the fuel from air injector into intake manifold; and (3) Air injector. This injector injects a mixture of fuel and air into intake port.

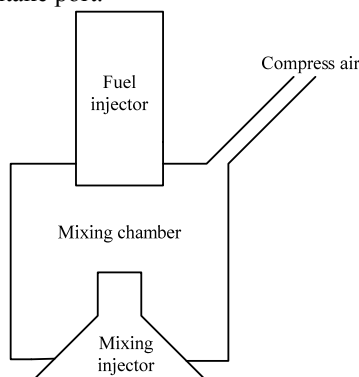


Fig. 1: Adapter of Air-assisted Injection System

To observe the spray behavior and atomization of air-assisted fuel injection, a system has been setup by using Fastec Imaging's Troubleshooter HR high-speed camera as shown in Fig. 2.

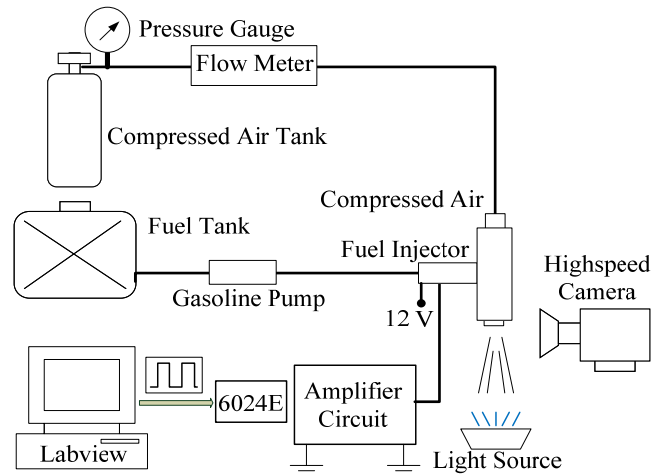


Fig. 2: Fuel Atomization Analyzing System

Fig. 3 shows the comparison of fuel atomization between original PFI injector and air-assisted injector. The original injector (Fig. 3a) has two holes. The two sprays inject into two intake ports during valve closing for evaporating before going into cylinder. The fuel drop size is larger. The Air-assisted injector (Fig. 3b) has better atomization which is injected through the intake port into cylinder during valve opening.

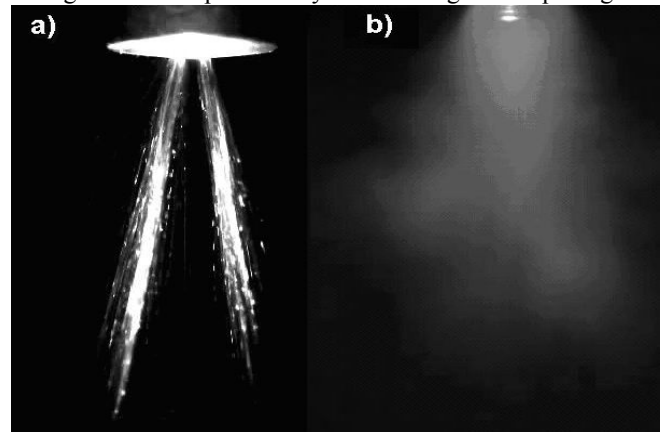


Fig. 3: Fuel spray photo: (a) original injector and (b) Air-assisted injector

### C. Swirl Generation

Swirl is defined as rotation of the charge about the cylinder axis. In order to assessing swirl in engine cylinders, the main issues concerned are firstly the techniques for measuring the flow and secondly, the method to calculate the data, which involves the definitions of 'Swirl Ratio'. The concepts of measurement method were shown in Fig. 4. They were measured on a steady flow bench Super Flow SF-120. A swirl adapter was designed based on the dimension of target engine to simulate the flow from the intake port into the cylinder. Paddle wheels were installed in the adapters to measure the charge motion revolution, as shown in Fig. 4.

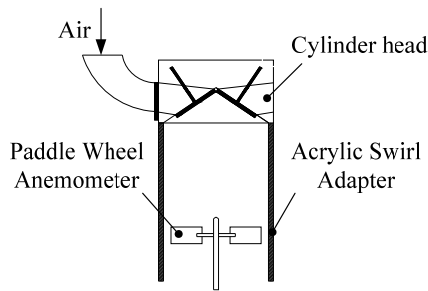


Fig. 4: Swirl measurement methods

The test engine had two intake ports without any swirl charge motion. In general, swirl can be induced by port geometry. When one of the intake ports was deactivated as shown in Fig. 5, the swirl ratio was increased to 2 ( $R_s=2$ ).

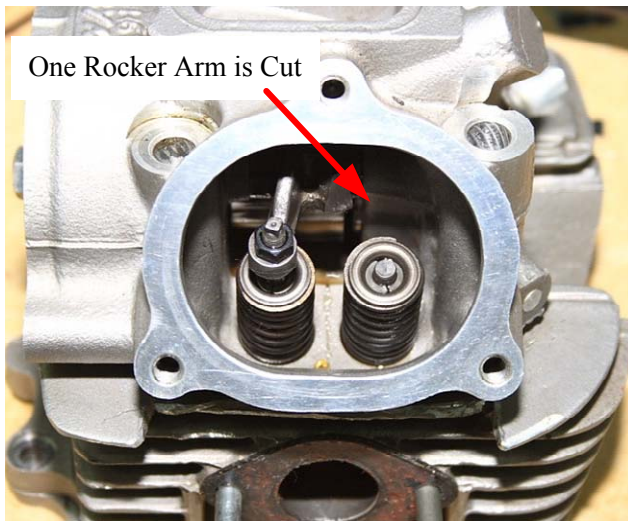


Fig. 5: Cylinder head with one intake valve closed

A swirl control plate, which was installed in intake port as shown in Fig. 6, was designed to increase the swirl ratio to 3.5 ( $R_s=3.5$ ).

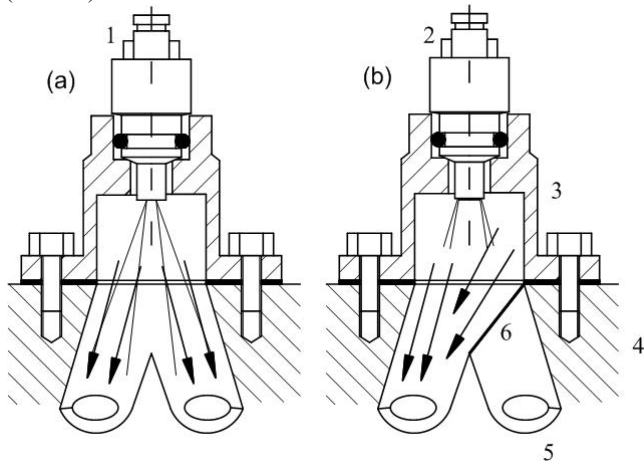


Fig. 7: Schematic of intake port: (a) original engine; (b) modified port for SDI engine. 1: Original injector (2 holes); 2: Air-assisted injector; 3: Intake manifold; 4: Cylinder head; 5: Deactivation port; and 6: Swirl control plate

#### D. Experimental Apparatus

The schematic diagram of the experiment setup is shown in Fig. 8. Engine experiment was performed by an Eddy-current engine dynamometer FE-150-S which has good adaptive with control accuracy is  $\pm 10\text{rpm}$  and  $\pm 0.4\%$  torque full scale. The fuel flow rate was measured by using ONO SOKKI FX-1110 mass burette flow detectors. Exhaust gases were measured by HORIBA MEXA-584L exhaust analyzer. A piezoelectric-typed 6051B KISTLER pressure transducer was located on the cylinder head. The pressure signal goes through KISTLER amplifier to become analog signal, and shows on AVL 619 Indicom. At the same time, instant crank angle was measured by BEI H25 encoder that is connected to crankshaft. The cylinder pressure was recorded every  $1^\circ\text{CA}$  for 100 cycles. The measured pressure data were then used for calculating the heat release rate.

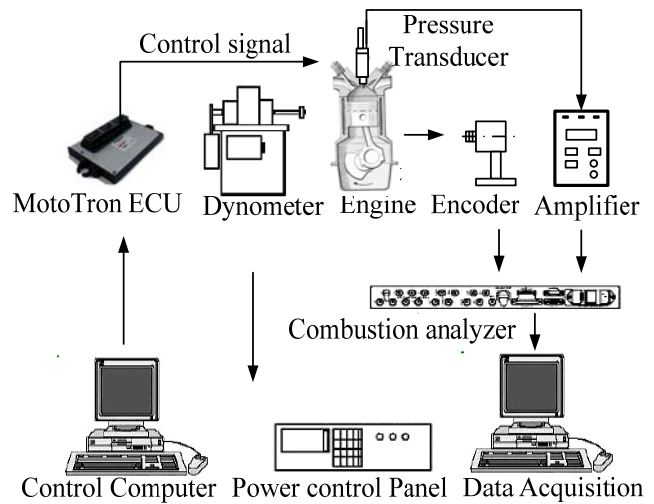


Fig. 8: Schematic diagram of experiment setup

Engine control was accomplished by using a MotoHawk ECU 555-80 controller produced by Woodward to control the fuel injection rate, injection timing, dwell, and ignition timing. The MotoHawk allows the user to automatically generate machine code from Simulink diagrams and to operate control hardware in real-time operation.

#### E. Experimental Approaches

At first, the CFD software was used to investigate the in-cylinder air motion of original port and modified swirl port. After that, experiments were performed on target engine through three different swirl ratios to study the combustion characteristics of swirl charge. The experiment of swirl ratio 0 was executed by using original PFI engine without baffle plate which means the mixture was formed by homogeneous charge. However, the SDI engine with higher swirl generation, air-assisted fuel injector, and injection during valve opening was utilized for the experiments of swirl 2 and 3.5.

After discussing the combustion characteristics of swirl charge, the lean limit was investigated and the minimum advance for best torque (MBT), fuel consumption, and emission with various excess air ratios ( $\lambda_s$ ) and swirl ratios were investigated as well. The experiments conducted the lean

limit tested at two conditions: 4500 rpm at throttle opening of the throttle position sensor (TPS) 13%, and 5300 rpm at TPS 29%. The operation condition of 4,500 rpm at TPS 13% (BMEP, Brake Mean Effective Pressure, 1.7 bar) was similar to the vehicle speed 30km/h and that of 5,300 rpm at TPS 29% (BMEP 2.5 bar) was similar to the vehicle speed 50 km/h.

The lean-limit of original engine was found by keeping the coefficient of cycle variation (COV) of indicated mean effective pressure (IMEP) within 10%. Ignition timing was controlled to get MBT. The lean-limit test of modified engine was taken by closing one port or using baffle plate, running the engine with the same conditions as original engine test but firstly, finding out the injection time which has good lean-limit and then decreasing more fuel to get better lean-limit.

The engine characteristic needs to have low fuel consumption at low load but good power at high load. Finally, the engine performance under low load and low engine speed was conducted from experiments by applying SDI. In addition, an ECE-40 driving pattern was used to study the fuel consumption and emissions of target vehicle with SDI engine as compared with original PFI engine.

### III. RESULTS AND DISCUSSION

#### A. In-Cylinder Air Motion

In truth, the in-cylinder swirl motion can not be examined easily. Virtual reality by using of computational fluid dynamics (CFD) software has been recognized as a simulation technique of high accuracy [12]. Therefore, CFD plays an important role in predicting the flow field characteristics, which was difficult to be observed [13]. The study used the ANSYS/FLUENT CFD software to investigate the in-cylinder air motion of non-swirl and swirl. The accuracy of simulation model which is used in CFD software is quite important, because that affects the simulation results directly. The cylinder head which includes intake and exhaust geometry is relatively a complex part to establish the model. Therefore, a model, obtained through 3-D scanning of a cylinder head of target engine, was employed in CFD simulation to reveal the practical characteristics from simulation results. The swirl ratio from CFD simulation was verified by the results from steady flow bench. As a result, the average error percentage was about 1.09%.

First of all, the air motion of original engine with homogeneous charge was simulated, which can be seen in Fig. 9. As can be seen from Fig. 9, it does not have swirl motion during intake process.

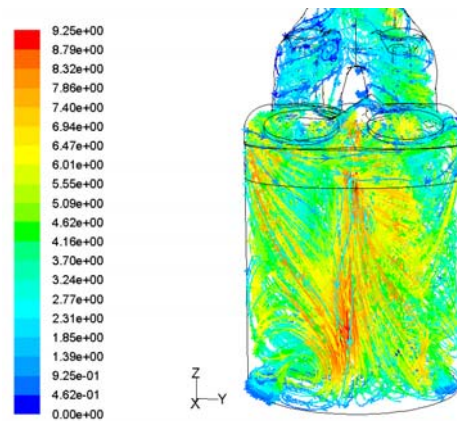


Fig. 9: CFD simulation result of original engine

The simulation results of swirl ratio 2 and 3.5 are shown in Fig. 10 and Fig. 11, respectively. It can be seen from Fig. 10, one intake port is always closed to increase the swirl ratio to 2. As a result, that produces swirl motion during intake process. Moreover, the swirl motion by using the baffle plate with swirl 3.5 is much stronger, which can be seen in Fig. 11.

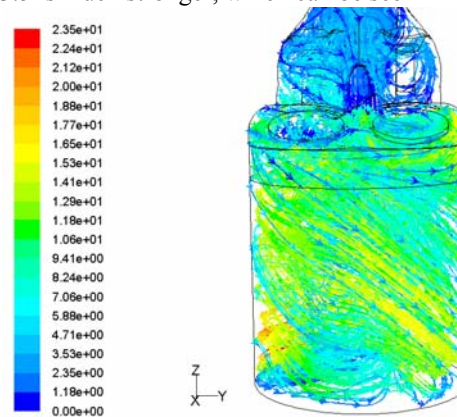


Fig. 10: CFD simulation result of swirl ratio 2

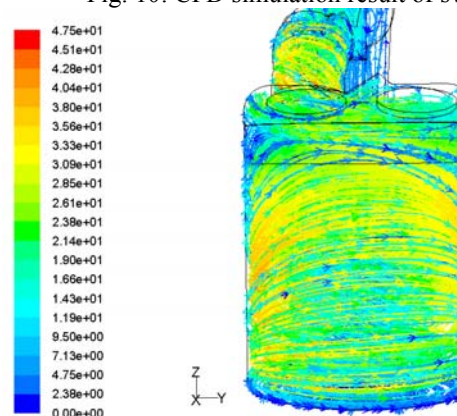


Fig. 11: CFD simulation result of swirl ratio 3.5

Higher swirl provides radial energies to keep the fuel, injected during the middle of intake stroke, on the upper location of cylinder which is so-called stratified charge, which can be seen in Fig. 12. That facilitates the mixture to be ignited even the excess air ratio is high.

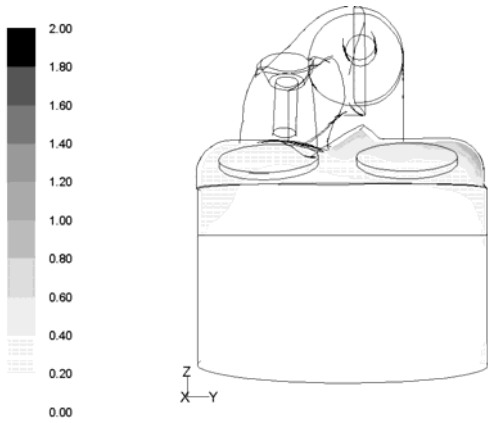


Fig. 12: In-cylinder fuel concentration of swirl ratio 3.5

**B. Combustion Characteristics**

The engine operating condition of 4500 rpm, excess air ratio 1.3, and 5300 rpm, excess air ratio 1.4 with three different swirl ratio were used to investigate the combustion characteristics of swirl charge. The spark timing was set at MBT; moreover, the start of injection timing of SDI was set at 80 °CA ATDC, which is near the middle of intake stroke. The heat release rate for air-cooled motorcycle engine is calculated by using the model developed by Wu et al. [14].

Fig. 13 and Fig. 14 show the heat release rate (HRR) of 4500 rpm and 5300 rpm, respectively. The HRR of SDI is higher than that of original engine ( $R_s=0$ ). It should be the effect of mixture stratification combined with swirl motion that remained more fuel concentration near the spark plug. Also high swirl motion implies high turbulent, which hastens the combustion reaction. The HRR of SDI engine (with  $R_s=3.5$ ) is the largest of these and that of original engine is smallest for both engine speeds.

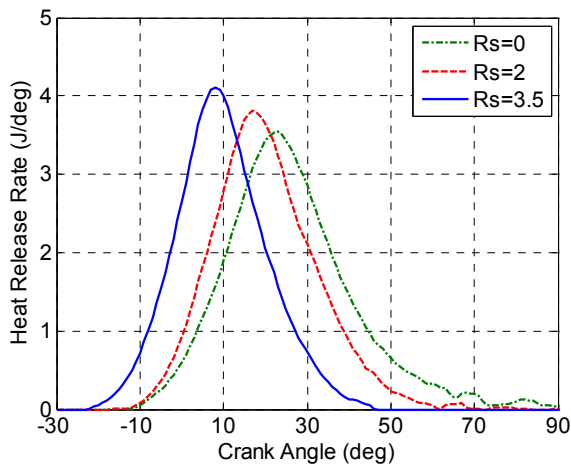


Fig. 13: Heat release rate at 4500 rpm, excess air ratio 1.3

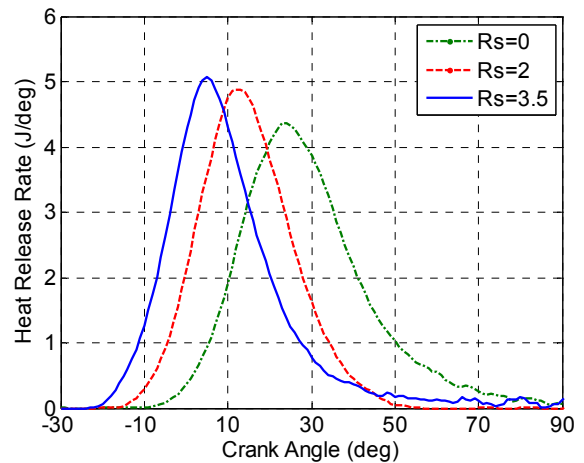


Fig. 14: Heat release rate at 5300 rpm, excess air ratio 1.4

It can also be seen from the cylinder pressure and rate of pressure rise; higher swirls induce faster combustion reaction, which results in higher rate of pressure rise and higher cylinder pressure. The rate of pressure rise and cylinder pressure are shown in Fig. 15 and Fig. 16 for 4500 rpm, and shown in Fig. 17 and Fig. 18 for 5300 rpm.

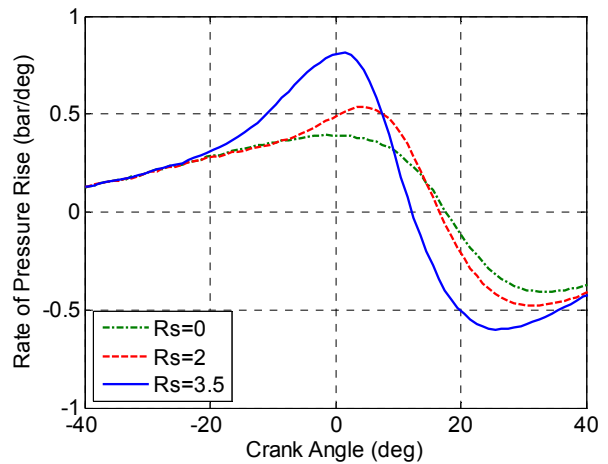


Fig. 15: Rate of pressure rise at 4500 rpm, excess air ratio 1.3

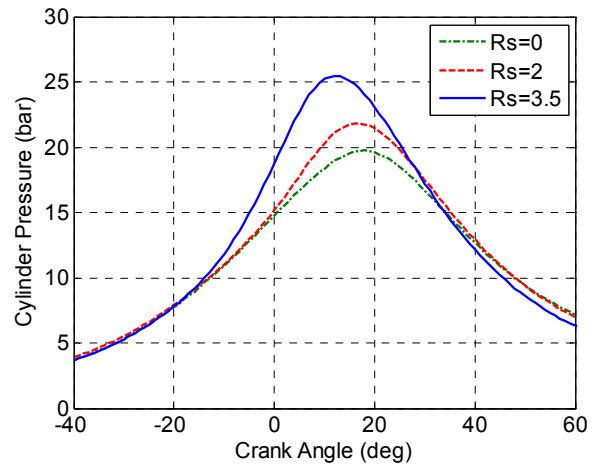


Fig. 16: Cylinder pressure at 4500 rpm, excess air ratio 1.3

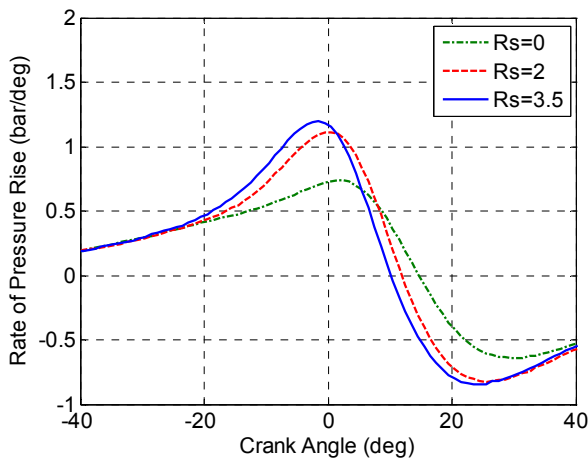


Fig. 17: Rate of pressure rise at 5300 rpm, excess air ratio 1.4

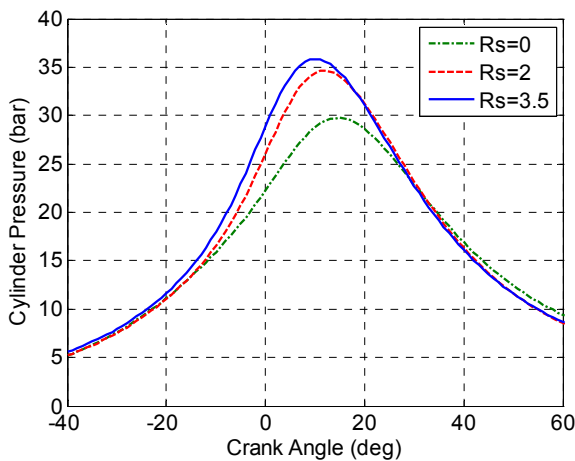


Fig. 18: Cylinder pressure at 5300 rpm, excess air ratio 1.4

Burn durations of rich mixture are faster than lean mixtures, which can be seen in Fig. 19. Because more fuel concentration will hasten the combustion reaction. Stephenv [10] pointed out that the flame speed seems to be a maximum at a slightly rich mixture and fall-off on other side. At low values of excess air ratio, the combustion process is both fast and stable so that swirl ratio has only a small impact on burn duration. With higher swirl ratios, most of fuel distributed near spark plug. Thus, it can be concluded that, higher swirl ratio will has best stratified and shorter burn duration.

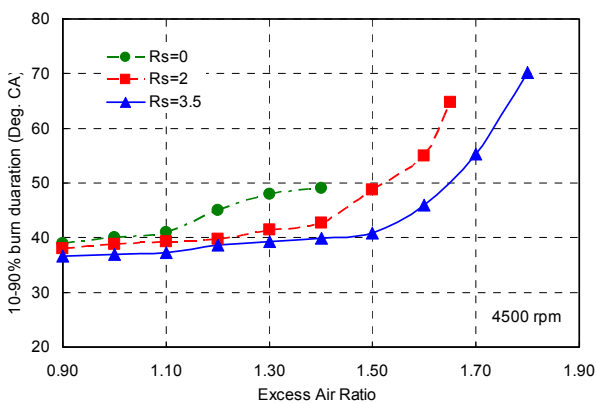


Fig. 19: 10-90% burn duration (°CA) vs.  $\lambda$  at 4500 rpm

### C. Lean Burn Ability for SDI Engine

Higher swirl can hasten the combustion reaction; moreover, the ignitibility of lean mixture can be improved by stratified charge. Therefore, the main conception of lean burn improvement is stratified charge by using swirl motion with fuel injection during valve opening. The first step of engine test is to find out the conformity injection timing with high swirl ratio. This experiment was performed by fixed engine speeds with precise TPS and excess air ratio ( $\lambda$ ). The test conditions were 4500 rpm at TPS 13% with excess air ratio 1.5 and 5300 rpm at TPS 29% with excess air ratio 1.6. The decisive factor of combustion stability is COV of IMEP. The injection timing was defined as the set off time for the start of injection. Fig. 20 shows that injection timing of SDI has much more influences on combustion stability. The injection timing at 80 °CA ATDC, which is near the middle of intake stroke, has lowest COV. Thus, this injection timing was taken for the overall SDI engine test. Fig. 20 also indicates that the best injection timing is not affected by engine speed as conclusion of Ohm et al. [11].

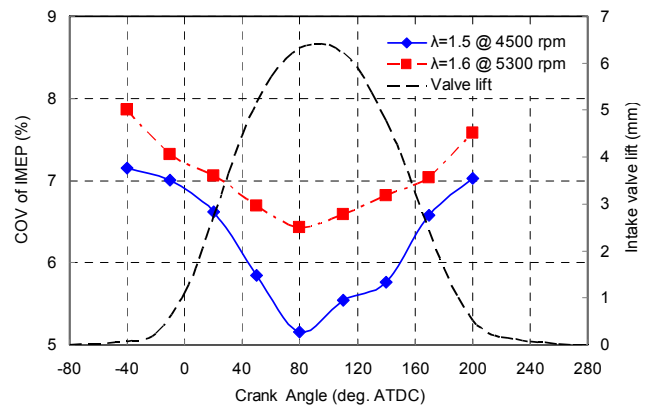


Fig. 20: Effect of injection timing on cycle variation

Fig. 21 and Fig. 22 show that the COV of IMEP for 100 cycles vs. excess air ratio ( $\lambda$ ) at 4500 rpm and 5300 rpm of using SDI engine as well as original engine. The COV value is limited as no more than 10% for evaluation lean-burn limit. Fig. 21 shows that COV of IMEP values are close at  $\lambda$  from 0.9 to 1.1. As mixtures become leaner, results of original engine (with  $R_s=0$ ) lean-limit is  $\lambda$  value approximately 1.3 for 4500rpm and 1.38 for 5300rpm. However, the SDI engine (with  $R_s=2$ ) can extend lean-limit to  $\lambda$  value 1.56 and SDI engine (with  $R_s=3.5$ ) can increase  $\lambda$  value up to 1.7 for 4500rpm (to 1.59 and 1.73 for 5300rpm), respectively. A homogeneous charge SI engine cannot achieve so lean. Therefore, it must have the effect of charge stratification.

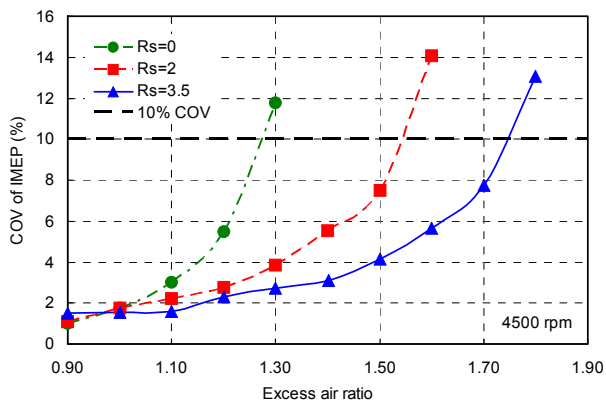


Fig. 21: COV of IMEP vs.  $\lambda$  at 4500 rpm

Increasing engine speed will increase turbulent intensity and extend lean-burn limit as the results for COV of IMEP at 5300rpm as shown in Fig. 22. For the  $\lambda$  less than 1.2, the COV of IMEP of three different swirl ratios are almost kept the same. As the  $\lambda$  becomes a little higher, the COV of IMEP keep close for both Rs=2 and Rs=3 until  $\lambda$  greater than 1.4. Consequently, the effect of swirl motion at lower engine speed is relatively important.

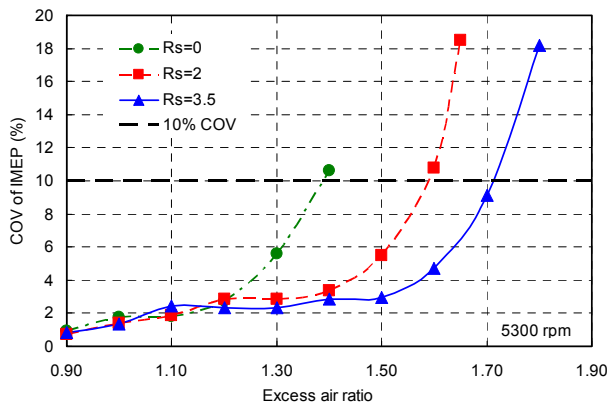


Fig. 22: COV of IMEP vs.  $\lambda$  at 5300 rpm

MBT timing is a familiar variable and is good indicators of relative lean burn limit and burn durations. Fig. 23 shows that the results for MBT spark timing vs. excess air ratio at 4500 rpm. MBT spark timing increases with increasing of engine speed and  $\lambda$  in all cases due to the slow burn of lean mixture. The MBT spark timing of original engine is always higher than that of SDI engine. This reason comes from stratified charge and swirl motion of SDI engine.

Without swirl, fuel is distributed at all area of combustion chamber where turbulence energy is low. Therefore, MBT timing value is higher than the one with swirl event which fuel was distributed near spark plug and flame propagated very quickly.

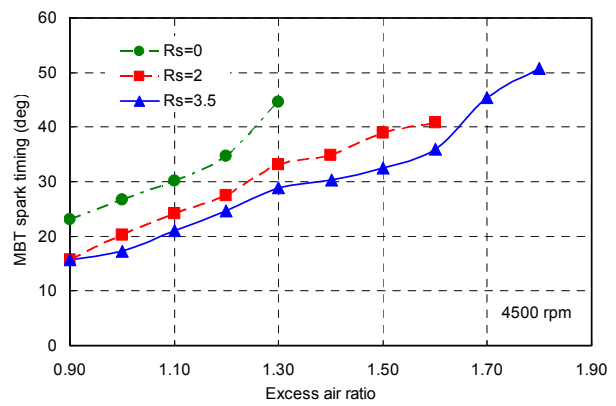


Fig. 23: MBT spark timing vs.  $\lambda$  at 4500 rpm

The brake specific fuel consumption (BSFC) is one of important parameter to present engine performance. It is also a measure of the engine's efficiency. Fig. 24 illustrates the relations of excess air ratio and the BSFC at 4500 rpm TPS 13%. The whole BSFC of SDI engine is lower than the original PFI engine. However, along with excess air ratio increased, combustion stability decreased, the lengthening burn duration and large cycle-by-cycle variation caused the BSFC to increase. The result is clear that SDI engine with high swirl charge motion has better fuel consumption than original engine at part load.

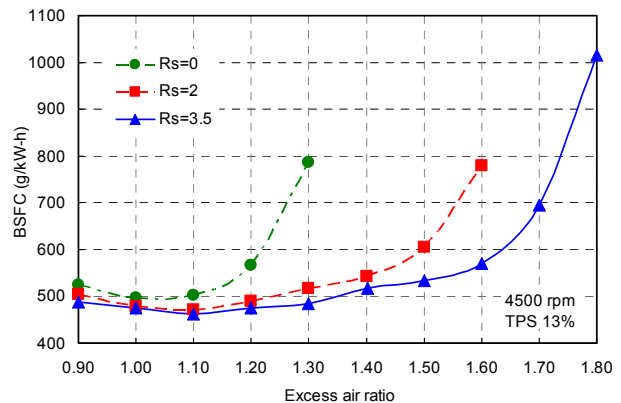


Fig. 24: BSFC vs.  $\lambda$  at 4500 rpm

Figs. 25-27 depict the effects of swirl motion on the exhaust emissions of engine. The rule of HC is the same as BSFC, which means at low values of excess air ratio from 0.9 to 1.25 (Fig. 25), HC emissions levels are low such as minimum values because of completely combustion. For still leaner mixtures, HC emissions rise more rapidly due to the increasing frequency of partial burning cycles. Instead of spreading the fuel droplet everywhere in the cylinder, the swirl motion provides air fuel mixture to be well mixed on the upper position of the cylinder. That is the reason that the HC emissions of using SDI engine are lower than original engine at each excess air ratio..

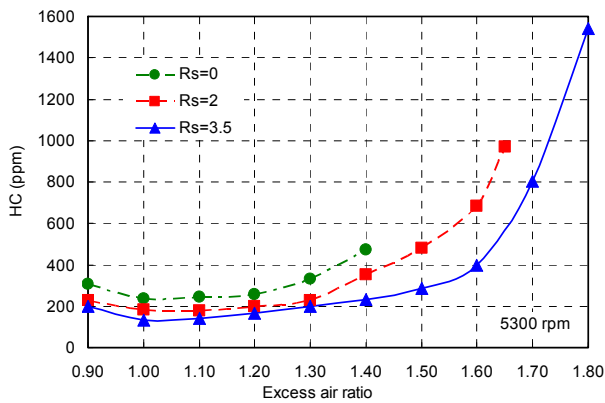


Fig. 25: HC emission (ppm) vs.  $\lambda$  at 5300 rpm

The results of carbon monoxide (CO) emissions vs. excess air ratio at 5300rpm TPS 29% is shown in Fig. 26. CO emissions quantity depended greatly on the excess air ratio, because this is the product of hydrocarbon reactions in the combustion process. Firstly, the carbon was associated with surplus oxygen to produce CO emissions. Then CO emissions will react with the surplus oxygen to produce CO<sub>2</sub>. Therefore CO emissions will reduce approximately constant at low levels of about 1% or less as seen in Fig. 26. The experiment investigated that with swirl ratios 2 and 3.5 of SDI engine, CO emissions concentration achieved lower than original engine even for the rich mixture. That is because the well-mixed mixture, caused by high swirl, can prevent incomplete combustion.

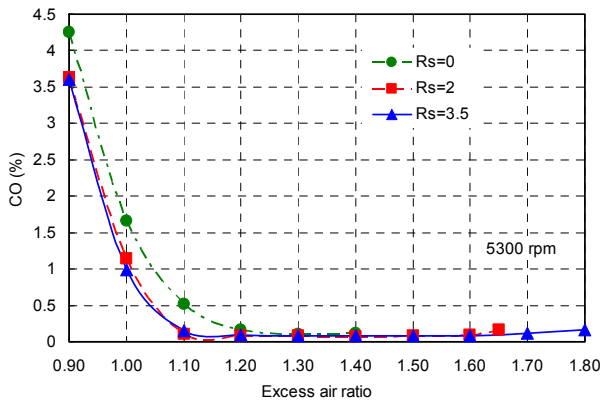


Fig. 26: CO emissions (%) vs.  $\lambda$  at 5300 rpm

Fig. 27 shows the NO<sub>x</sub> emission of using SDI engine with high swirl ratio as compared with original engine. The results show that the NO<sub>x</sub> emissions reach its maximum value at a little leaner from stoichiometric air fuel ratio. Also, the NO<sub>x</sub> emissions of high swirl are higher than original engine. In truth, the NO<sub>x</sub> formation mainly depends on the in-cylinder O<sub>2</sub> concentration and high combustion temperature. The combustion temperature of SDI method is higher due to well-mixed mixture that induces completely combustion.

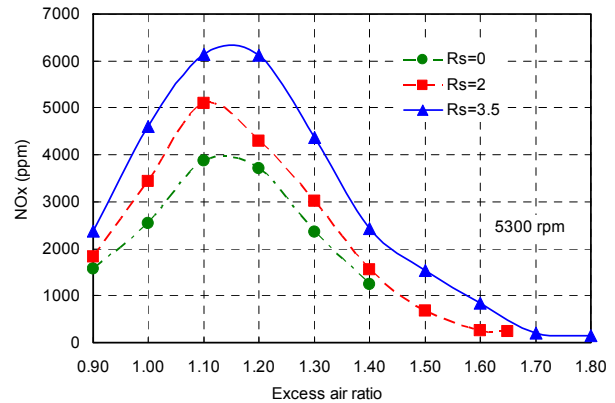


Fig. 27: NO<sub>x</sub> emissions (ppm) vs.  $\lambda$  at 5300 rpm

#### D. Driving Cycle Simulation

The motorcycle emission regulations of many countries follow ECE-40 driving cycle. In order to investigate the SDI engine performance on a motorcycle, this study used a driving cycle of ECE-40 to study the fuel consumption and emissions of the target motorcycle.

The engine operation points of the target 125cc motorcycle to accomplish the ECE-40 driving cycle test was calculated, which is shown in Fig. 28. The square line in Fig. 28 is located at the area of engine speed from 3500 to 5500 rpm and BMEP from 1.5 to 4 bar. That consists most of ECE-40 operating points. Therefore, the experiments of SDI engine performance map were executed inside this area, i.e. engine speed from 3500 to 5500 rpm with step of 500 rpm and BMEP from 1.5 to 4 bar with step of 0.5 bar. As a result, for the SDI engine, it operates at SDI mode within the engine speed from 3500 to 5500rpm and BMEP from 1.5 to 4 bar; however, it operates at original port fuel injection mode beside the area.

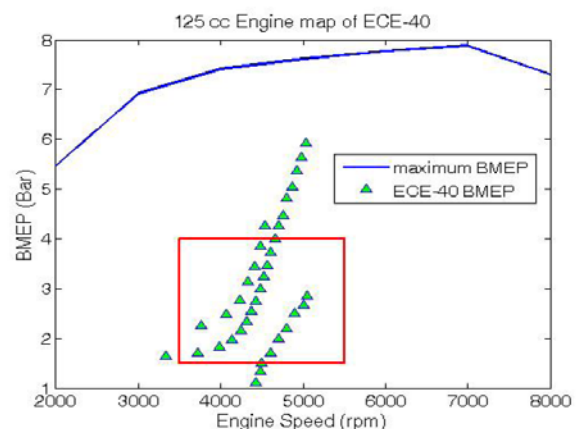


Fig. 28: Engine map of ECE-40 cycle

For the purpose to investigate the fuel consumption and emissions of target vehicle, the engine operation points which was taken from original engine performance map, includes BSFC, BSCO, BSHC, and BSNO<sub>x</sub>, was used for ECE-40 driving cycle simulation. Moreover, the SDI engine performance map which used the original engine performance map by substituting the operation points obtained by SDI experiments was used for ECE-40 driving cycle simulation as

well.

Fig. 29 shows the accumulative fuel consumption of original engine and SDI engine by calculating and summing all the fuel consumption results of each engine operation point which is used in ECE-40 driving cycle, respectively. The SDI operation duration indicates that the SDI engine is shifted to SDI mode operation. It can be seen from Fig. 29, when the SDI engine operates at original PFI mode, the fuel consumption keeps the same with original engine. However, the fuel consumption of SDI engine becomes lower while it operates in SDI mode. Consequently, the total fuel consumption of SDI engine is improved by 4% due to the lean burn ability of SDI mode.

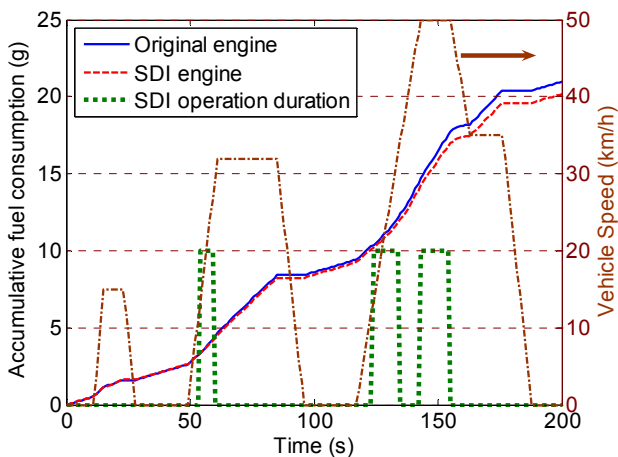


Fig. 29: Accumulative Fuel consumption from ECE-40 driving cycle calculation

Figs. 30-32 show the accumulative emissions of the target vehicle to accomplish the ECE-40 driving cycle simulation with original engine and SDI engine. As can be seen from Fig. 30, the CO formation rate of the SDI engine with SDI mode becomes lower. That is because the SDI mode provides high swirl motion which helps the air-fuel mixture to be well mixed, that can prevent incompletely combustion. Furthermore, the SDI engine operates with lean burn at SDI mode which means less quantities of hydrocarbon are reacted. As predicted, the total CO emission of SDI engine is improved by 31.1%.

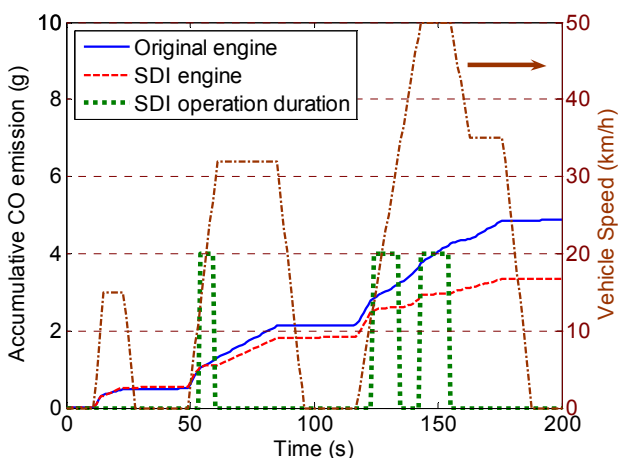


Fig. 30: Accumulative CO emission from ECE-40 driving cycle calculation

Fig. 31 shows the accumulative HC emission of ECE-40 driving cycle simulation. The HC emissions of using SDI engine with SDI mode are higher. The reason is that the SDI engine operates with lean mixture at SDI mode which results in increasing frequency of partial burning cycles; on the contrary, the original engine is always operated with the excess air ratio smaller than or equal to 1. The total accumulative HC emission of SDI engine is increased by 25%. However, it can be handled by post-treatment.

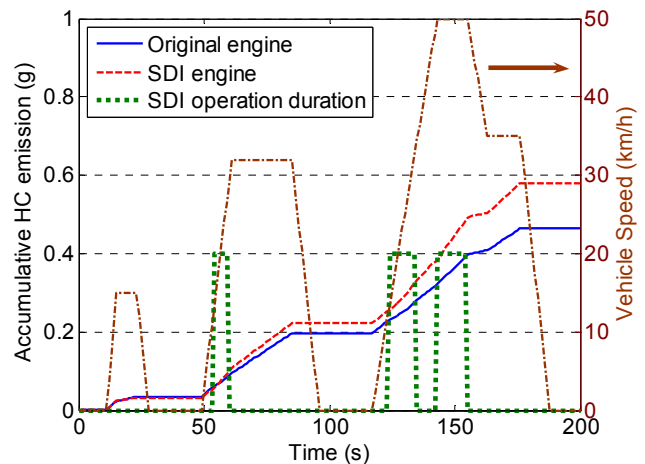


Fig. 31: Accumulative HC emission from ECE-40 driving cycle calculation

Wu et al. [15] had evaluated the circumstance of achieving the regulation by testing 49 of the most popular motorcycles in the market. Results show that the NOx regulation is the most difficult to achieve. Fig. 32 shows the accumulative NOx emission of target motorcycle after accomplish the simulation of ECE-40 driving cycle. The result shows that the SDI engine with SDI mode can reduce the NOx formation rate. That is because the combustion temperatures of SDI mode with lean mixture combustion are lower. Consequently, the total NOx emission of SDI engine is improved by 5.9%.

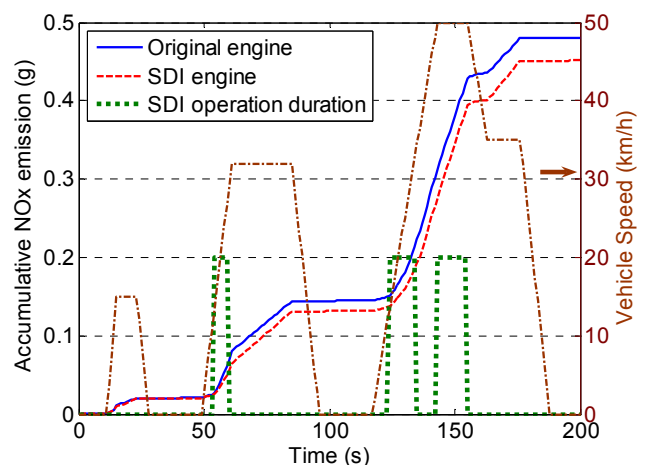


Fig. 32: Accumulative NOx emission from ECE-40 driving cycle calculation

## IV. CONCLUSION

This study focused on operating the SDI on a motorcycle engine with high swirl charge. Swirl ratio of in-cylinder air motions was increased by using two methods. The CFD software was employed to investigate the in-cylinder air motion of non-swirl and swirl. Experiments were performed to investigate the combustion characteristics of swirl charge. In addition, the lean burn ability for SDI engine was studied as well. After that, the SDI engine performance map which include the engine speed from 3500 to 5500rpm and BMEP from 1.5 to 4 bar was done and used for ECE-40 driving cycle simulation to investigate the fuel consumption and emissions of target vehicle. From the experiments results, it has been concluded:

1 - Using high swirl of charge motion, optimum fuel injection timing during intake valve opening, and using air-assisted injector to get better atomization of fuel spray are three main factors to develop SDI engine.

2 - The simulation results of CFD show that the higher swirl provides radial energy to keep the fuel, which is injected on the middle of intake stroke, around spark plug to increase lean-limit simultaneously.

3 - The optimal injection timing at 80 °CA ATDC, which is near the middle point of intake stroke, is the best point for SDI engine.

4 - The homogeneous charge of original (PFI) engine cannot achieve so lean. Increasing swirl ratio will increase burn rate and extend lean-limit of SDI engine up to 1.73 of excess air ratio, and it decreases cycle variation, ignition delay, BSFC, and HC emissions simultaneously.

5 - The simulation results of ECE-40 driving cycle show that by using SDI mode at low load operation, the fuel consumption, CO emission, and NOx emission were improved by 4%, 31.1%, and 5.9%, respectively. However, the HC emission was increased by 25%. However, it can be handled by post-treatment.

6 - It can be identified from the simulation results of ECE-40 driving cycle, the effects of swirl ratio on stratified charge were one of the most promising methods to increase engine performance and decrease the fuel consumption at part load for motorcycle. Thus, SDI engine is a possibility application for motorcycle engine in feasibility.

## ACKNOWLEDGMENT

The authors would like to thank the National Science Council (NSC, Taiwan, ROC) for financial support (NSC-96-2221-E-027-037-MY3).

## REFERENCES

- [1] CH. Satyanarayana and P. V. Rao, "Influence of key properties of pongamia biodiesel on performance combustion and emission characteristics of a DI diesel engine," *WSEAS Trans. on Heat and Mass Transfer*, vol. 4, pp. 34-44, April 2009.
- [2] C. Arapatsakos, D. Christoforidis, G. Sarantitis, and D. Giannopoulos, "Fuel mixtures of diesel-maize oil," *International Journal of Energy*, vol. 2, pp. 43-50, 2008.
- [3] C. Arapatsakos, D. Christoforidis, A. Karkanis, and K. Mitroulas, "Fuel of diesel-olive seed oil mixtures," *International Journal of Energy*, vol. 2, pp. 35-42, 2008.
- [4] C. Yu, T. Kim, Y. Yi, J. Lee, S. Noh, and K. Choi, "Development of KMC 2.4L lean burn engine," *SAE Technical Paper Series*, No. 950685, 1995.
- [5] A. A. Quader, "Lean combustion and the misfire limit in spark ignition engines," *SAE Technical Paper Series*, No. 741055, 1974.
- [6] C. Brehm, J. H. Whitelaw, L. Sassi, and C. Vafidis, "Air and fuel characteristics in the intake port of a SI engine," *SAE Technical Paper Series*, No. 1999-01-1491, 1999.
- [7] M. Fry, J. King, and C. White, "A comparison of gasoline direct injection systems and discussion of development techniques," *SAE Technical Paper Series*, No. 1999-01-0171, 1999.
- [8] J. Jarosinski, R. Lapucha, J. Mazurkiewicz, and S. Wojcicki, "Combustion system of a lean-burn piston engine with catalytic prechamber," *SAE Technical Paper Series*, No. 2001-01-1186, 2001.
- [9] D. Plohberger, L. A. Mikulic, and K. Landfahrer, "Development of a fuel injected two-stroke gasoline engine," *SAE Technical Paper Series*, No. 880170, 1988.
- [10] R. Stephen, *An introduction to combustion*, McGraw-Hill, pp. 29, 2000.
- [11] I. Y. Ohm and Y. S. Cho, "Mechanism of axial stratification and its effect in an SI engine," *SAE Technical Paper Series*, No. 2000-01-2843, 2000.
- [12] J. C. Park and K. S Kim, "Numerical simulations of fully nonlinear wave motions in a digital wave tank," *Proceedings of the 5<sup>th</sup> WSEAS Int. Conf. on System Science and Simulation in Engineering*, Tenerife, Canary Islands, Spain, December 16-18, 2006.
- [13] S. M. E. Haque, M. G. Rasul, A. Deev, M. M. K. Khan, and J. Zhou, "Numerical simulation of turbulent flow inside the electrostatic precipitator of a power plant," *Proceedings of the 2006 WSEAS/ASME Int. Conf. on Fluid Mechanics*, Miami, Florida, USA, pp. 25-30, January 18-20, 2006.
- [14] Y. Y. Wu, B. C. Chen, and F. C. Hsieh, "Heat transfer model for small-scale air-cooled spark-ignition four-stroke engines," *International Journal of Heat and Mass Transfer*, Vol. 49, pp. 3895-3905, 2006.
- [15] K. T. Wu et al., "The 5<sup>th</sup> stage motorcycle emission standard and low emission motorcycle technology evaluation," *Environmental Protection Administration of Taiwan, ROC*, Project number: EPA-93-FA13-03-A158.